AJNR

Efficacy of DynaCT Digital Angiography in the Detection of the Fistulous Point of Dural Arteriovenous Fistulas

T. Hiu, N. Kitagawa, M. Morikawa, K. Hayashi, N. Horie, Y. Morofuji, K. Suyama and I. Nagata

AJNR Am J Neuroradiol 2009, 30 (3) 487-491
doi: https://doi.org/10.3174/ajnr.A1395
http://www.ajnr.org/content/30/3/487

ORIGINAL RESEARCH

Efficacy of DynaCT Digital Angiography in the Detection of the Fistulous Point of Dural Arteriovenous Fistulas

T. Hiu
N. Kitagawa
M. Morikawa
K. Hayashi
N. Horie
Y. Morofuji
K. Suyama
I. Nagata

BACKGROUND AND PURPOSE: Identifying the precise hemodynamic features, including the fistulous point, is essential for treatments of dural arteriovenous fistulas (DAVFs). This study illustrates the efficacy of DynaCT digital angiograms obtained from a 3D C-arm CT to directly visualize the location of the fistulous points in DAVFs.

MATERIALS AND METHODS: This retrospective study observed 14 consecutive patients with DAVFs, which included 7 cavernous sinuses, 4 transverse-sigmoid sinuses, 2 convexity-superior sagittal sinuses, and 1 tentorial sinus. In the assessment of the practical applicability for the diagnosis of DAVFs, images obtained from 2D digital subtraction angiography (DSA) and DynaCT were comparatively evaluated.

RESULTS: In all patients, DynaCT digital angiography could clearly demonstrate the feeding arteries, the fistulous points, and the draining veins. Significant anatomic landmarks for the fistulous points with relationships to osseous structures were also provided. Compared with 2D DSA, DynaCT digital angiograms demonstrated 12 additional findings in 8 patients (57%), including the detection of the fistulous points ($n = 7$), the feeders ($n = 1$), the retrograde leptomeningeal drainage ($n = 1$), the draining veins ($n = 1$), and the venous anomaly ($n = 2$).

CONCLUSIONS: In comparison with 2D DSA, DynaCT may provide more detailed information to evaluate DAVFs. DynaCT digital angiograms have a high contrast and isotropic spatial resolution, allowing a reliable visualization of small vessels and fine osseous structures. Such detailed information, especially for the location of the fistulous points, could be very useful for either the endovascular or the surgical treatments of DAVFs.

Dural arteriovenous fistulas (DAVFs) comprise 10% to 15% of intracranial arteriovenous malformations.[1-3] Various modalities have been applied to treat DAVFs, including endovascular procedures,[4] direct sinus packing,[5] surgical interruption of the draining veins,[5] gamma knife surgery,[6] and combinations of these treatments.[7,8] The treatment strategy is based on the angiographic features, the severity of presenting symptoms, and the patient's condition.[9] Therefore, the identification of the precise hemodynamic features with regard to the feeding arteries, the draining veins, and especially the location of the fistulous points is essential for the optimal treatments of DAVFs.

Although numerous imaging techniques have been applied for the detection of DAVFs,[10,11] MR imaging was found to have a limited ability to demonstrate anatomic details of DAVFs. Currently, digital subtraction angiography (DSA) remains the criterion standard to evaluate the hemodynamic features. However, 2D DSA may not clearly delineate the fistulous point without performing subsequent selective angiographic examinations.

We herein report the usefulness of a modified 3D C-arm-mounted flat-panel detector (FPD) cone-beam CT system, DynaCT digital angiography (Siemens, Erlangen, Germany), which is generated from unsubtracted rotational images. DynaCT allows volumetric data acquisition in a single rotation of the source and the detector.[12] To assess the practical applicability for diagnosis of DAVFs, we comparatively evaluated images obtained from 2D DSA and DynaCT.

Received May 16, 2008; accepted after revision October 3.

From the Departments of Neurosurgery (T.H., N.K., K.H., N.H., K.S., I.N.) and Radiology (M.M.), Nagasaki University Graduate School of Biomedical Sciences, Nagasaki, Japan.

Please address correspondence to Takeshi Hiu, MD, Department of Neurosurgery, Nagasaki University Graduate School of Biomedical Sciences, 1-7-1 Sakamoto, Nagasaki 852-8501, Japan; e-mail: thiu-nagasaki@umin.ac.jp

DOI 10.3174/ajnr.A1395

Materials and Methods

Between August 2006 and February 2008, a total of 14 consecutive patients (5 men and 9 women; age range, 58–86 years; mean [SD], 71.7 ± 7.4 years) in this hospital were confirmed to have DAVFs. DAVFs included 7 cavernous sinuses (CSs), 4 transverse-sigmoid sinuses, 2 convexity-superior sagittal sinuses, and 1 tentorial sinus. All patients underwent 2D DSA and 3D rotational angiography. Angiography was performed with a biplane FPD angiographic suite (AXIOM Artis dBA; Siemens). 2D DSA was performed after catheterization of the common, external, and internal carotid arteries and catheterization of the dominant vertebral artery. We performed 3D rotational angiography using a C-arm mounted FPD system and the following parameters: 5-second rotation; rotation angle, 190° with 1.5° increment revealing 126 projections; 1240 × 960 matrix in projections at zoom 0 after resampling; a small focal spot size; rotation speed, 38°/s; frame rate, 25.2 frames/s; and pulse dose, 0.36 μGy/p. The volumes of nonionic iodinated contrast agent (Iopamiron 300; Bayer HealthCare, France) and the injection rates were 14 mL and 2 mL/s, respectively, to the external carotid artery (ECA) and 19 mL and 3 mL/s, respectively, to the internal carotid artery (ICA). We then reconstructed and analyzed the filling run volume using a dedicated commercially available workstation (syngo X-Workplace). DynaCT images then consisted of thin-section maximum intensity projections (MIPs).

All patients underwent appropriate endovascular treatments (transarterial or transvenous embolization). The imaging quality of

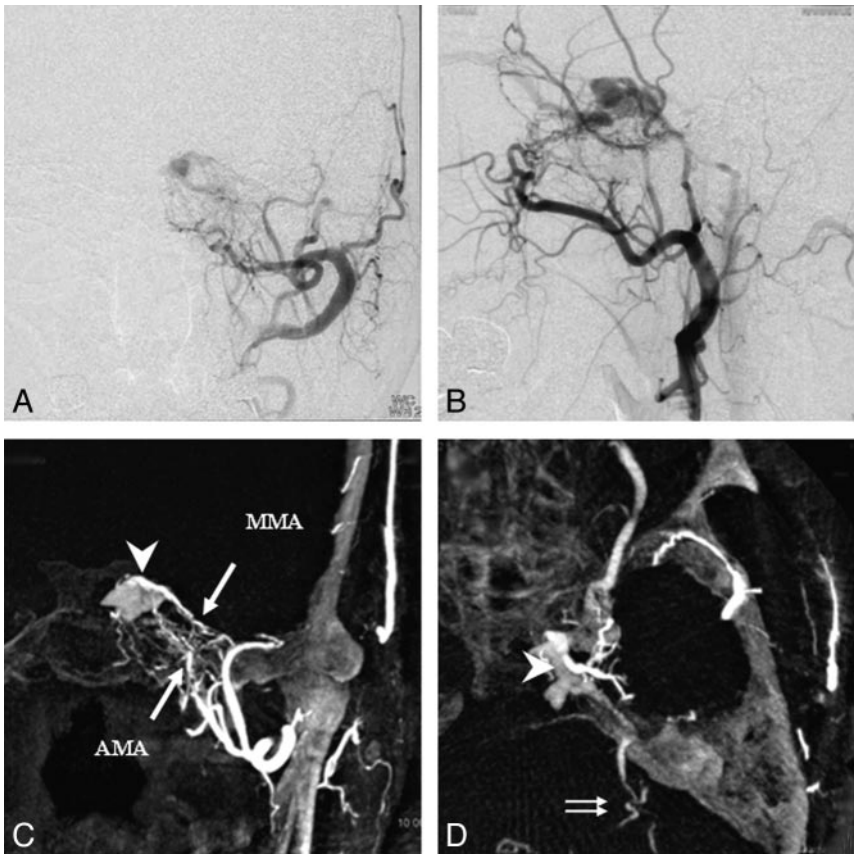

Fig 1. Case 4, a 68-year-old man with a left CS DAVF. *A* and *B,* 2D DSA shows the left CS DAVF draining into the SOV, the SPS, and the IPS. *C* (*coronal image*) and *D* (*axial image*), DynaCT shows a DAVF supplied by the AMA and the MMA (*arrows*). The fistulous point is located in the posterosuperior compartment of the left CS (*arrowhead*), and the left SPS drains to the left petrosal vein with cortical venous reflux (*double arrows*).

the hemodynamic features including the feeding arteries, the location of the fistulous points, and the draining veins was comparatively evaluated between 2D DSA and DynaCT digital angiography. The location of the fistulous points of CS DAVFs was classified as one of 3 types: medial, anteroinferior, and posterosuperior according to the relationship of each venous compartment to the ICA.[13] Tentorial DAVFs were categorized focusing on the location in the tentorium as follows: tentorial marginal type; tentorial lateral type; and tentorial medial type, according to the Picard classification.[14] The fistulous points were defined as detected when the location and the range of the fistulous points were precisely demonstrated. The feeding arteries and the draining veins were defined as detected only when all the vessels were demonstrated.

Results

In all patients, DynaCT digital angiography could clearly demonstrate the feeding arteries, the fistulous points, and the draining veins. Significant anatomic landmarks for the fistulous point with relationships to surrounding structures were also provided. Compared with 2D DSA, DynaCT digital angiograms demonstrated 12 additional findings in 8 patients (57%), including the detection of the fistulous points ($n = 7$; Fig 1–3), the visualization of the feeders ($n = 1$), the visualization of the retrograde leptomeningeal drainage ($n = 1$; Fig 1), the visualization of the draining veins ($n = 1$), and the delineation of the venous anomaly ($n = 2$, sphenopetrosal sinus; Fig 2 and fenestration of confluence). The information obtained from DynaCT was considered to be useful during manipulations of endovascular treatments in 5 (36%) of 14 DAVFs (Fig 1–3). No complications were observed during the procedures of 2D DSA and DynaCT imaging.

Representative Cases

Case 4. A 68-year-old man presented with diplopia. 2D DSA showed the presence of a DAVF with the primary supply from the right internal maxillary artery (IMA), the ascending pharyngeal artery (APA), the accessory meningeal artery (AMA), the middle meningeal artery (MMA), and the meningohypophyseal trunk (MHT), draining into the left superior ophthalmic vein (SOV), the superior petrosal sinus (SPS), and the inferior petrosal sinus (IPS; Fig 1 *A, B*). DynaCT digital angiography with the injection of the right ECA clearly demonstrated the fistulous point in the posterosuperior compartment of the left CS (Fig 1*C*). The SPS drained to the left petrosal vein with cortical venous reflux (Fig 1*D*). Transvenous embolization with fiber coils was performed via the right IPS. After selective occlusion of the retrograde venous drainage outflows (SPS and SOV) as the initial step, the posterosuperior compartment of the right CS was mainly packed with coils, which resulted in a complete obliteration of the DAVF. DynaCT was beneficial for visualization of the retrograde leptomeningeal drainage and the location of the fistulous points in the posterosuperior compartment of the right CS.

Case 7. A 73-year-old woman presented with diplopia. 2D DSA showed the presence of a DAVF with the primary supply

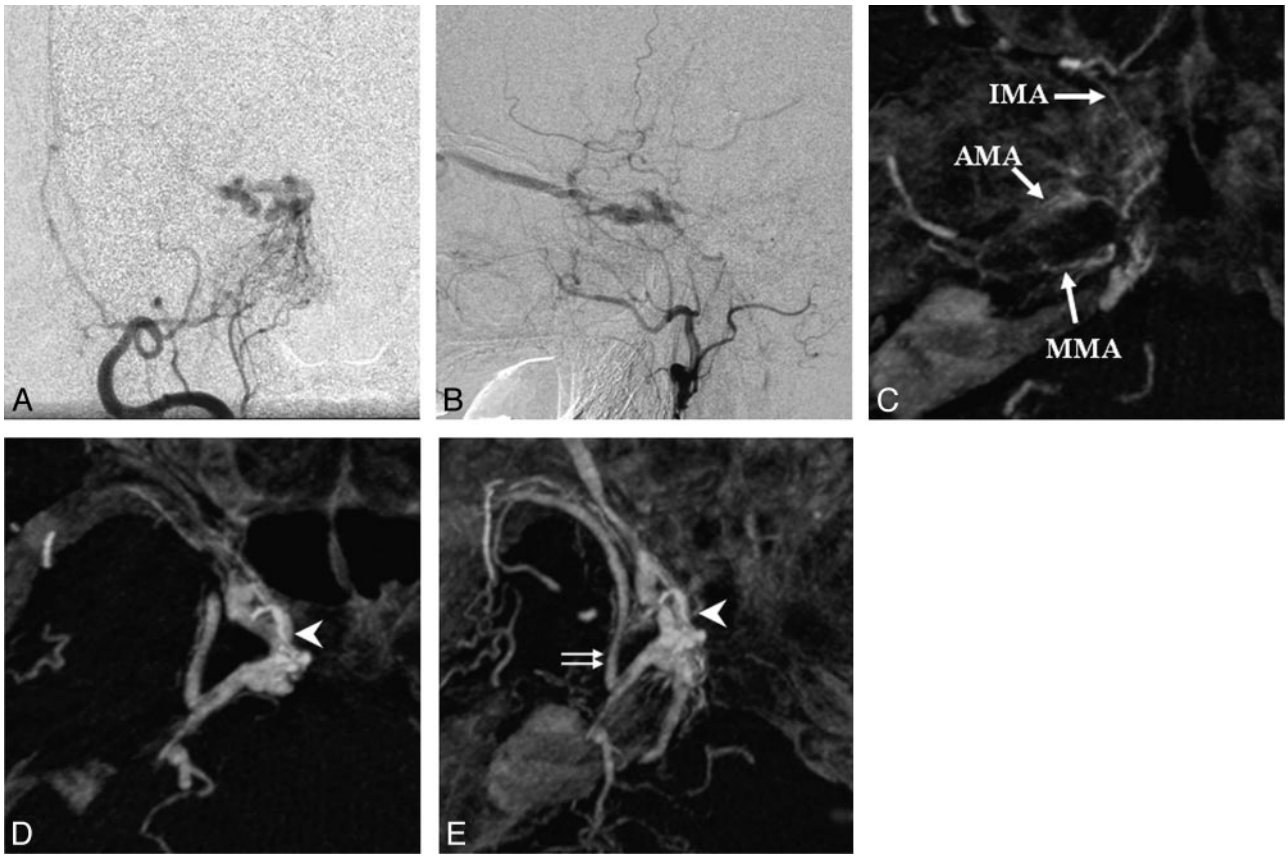

Fig 2. Case 7, a 73-year-old woman with a right CS DAVF. *A* and *B*, 2D DSA shows the right CS DAVF draining into the SOV, the SPS, and the IPS. *C–E* (*axial images*), DynaCT shows a DAVF supplied by the IMA, the AMA, and the MMA (*arrows*). The fistula is located in the medial compartment of the right CS (*arrowhead*), and the right SPS is connected to the superficial middle cerebral vein (ie, the sphenopetrosal sinus; *double arrows*).

from the right IMA, the AMA, the MMA, the APA, and the MHT, draining into the right SOV, the SPS, and the IPS (Fig 2*A, B*). DynaCT digital angiography with injection of the right ECA clearly demonstrated the fistulous point to be in the medial compartment of the right CS (Fig 2*C–E*), and the right SPS was connected to the superficial middle cerebral vein (ie, the sphenopetrosal sinus). Transvenous embolization with fiber coils was performed via the right IPS. After the selective occlusion of the retrograde venous drainage outflows (SPS and SOV) as the initial step, the medial compartment of the right CS was mainly packed with coils, which resulted in a complete obliteration of the DAVF. DynaCT precisely delineated the location of the fistulous points in the medial compartment of the right CS and the venous anomaly. The detection of the sphenopetrosal sinus contributed to the selective occlusion of the SPS and SOV as the initial step.

Case 10. A 58-year-old man presented with a headache and right-sided dysmetria. MR diffusion-weighted imaging demonstrated a hyperintense area within the right cerebellar hemisphere. 2D DSA showed a presence of a DAVF with the primary supply from the right APA and the bilateral occipital arteries (OAs; Fig 3*A, B*). DynaCT digital angiography with the injection of the right ECA clearly demonstrated the location of the fistulous point in the right medial tentorium and the veins draining into the inferior hemispheric veins with varix formation (Fig 3*C–F*). The fistulous point was successfully obliterated by deposition of *n*-butyl-2-cyanoacrylate into the fistula via the distal APA of the fistulous point nearby (Fig 3*G–H*). DynaCT was beneficial for several reasons. By adjusting the relative opacity of the adjacent occipital bone, the site of the fistula was identified in the medial tentorium without superselective catheterization of the external branches of the ECA. It was retrogradely drained into the leptomeningeal veins with varix formation. That information from the DynaCT digital angiograms in this case enabled the interventionalist to select the APA most feasibly to embolize, and to better understand how to safely navigate the feeding vessel.

Discussion

Currently, the treatment of DAVFs primarily involves an endovascular approach in which identification of the precise hemodynamic features is essential. It seems quite important to detect the location of the fistulous points because their complete obliteration could result in an anatomic and a clinical cure. In radiographic analyses, conventional CT and standard MR imaging are of limited value for the diagnosis and the classification of DAVFs.[15] In our study, MR DSA did not show all of the anatomic details of DAVFs, though it may be able to identify important hemodynamic abnormalities related to the risk for hemorrhaging.[11] 3D time-of-flight MR angiography has been reported to allow the visualization of an abnormal arterial flow and static venous anomalies, but the fistula has been difficult to identify.[10,16]

In general, DSA has a sole diagnostic value for the hemodynamic evaluation despite its invasiveness and periprocedural complications.[17,18] Oblique projections of 2D DSA and

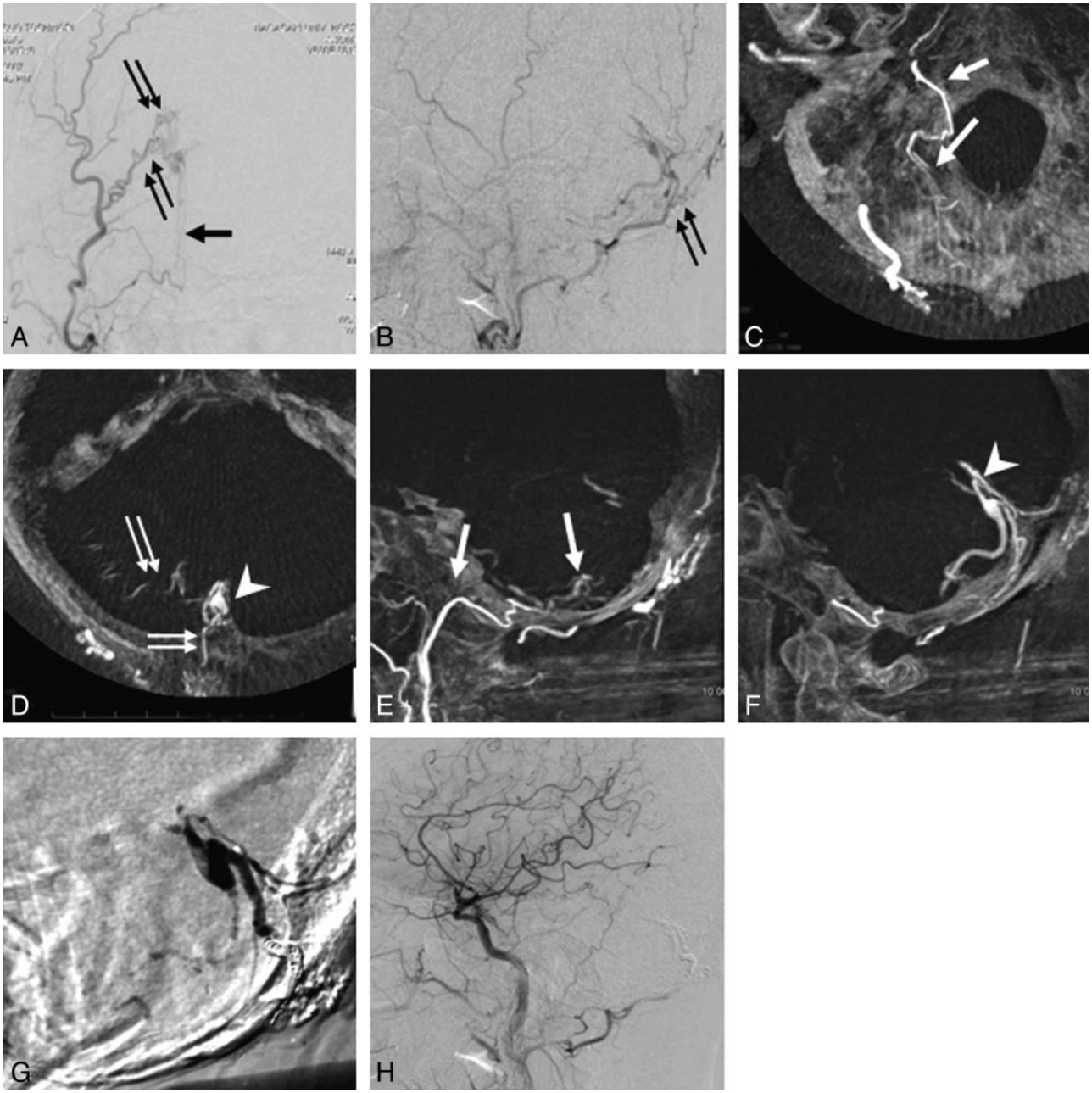

Fig 3. Case 10, a 58-year-old man with a tentorial DAVF. *A* and *B,* 2D DSA shows a DAVF supplied by the APA and the OA. *C* and *D* (*axial images*) and *E* and *F* (*sagittal images*), DynaCT shows a DAVF supplied by the APA (*arrow*) and OA (*double arrows*) draining into the inferior hemispheric vein. The fistula is located in the medial tentorium (*arrowhead*). *G,* Injection of *n*-butyl-2-cyanoacrylate into the fistula from the distal APA. *H,* 2D DSA shows a complete obliteration of the DAVF.

repeated selective angiography require high doses of contrast material, long examination times, and substantial exposure to radiation.[19] DynaCT digital angiography could contribute to minimize these disadvantages of conventional DSA because it is designed to enhance the 3D interpretation of conventional DSA without various oblique projections or selective angiography, despite a relatively long period (approximately 4 minutes) required to produce the images. 3D DSA has recently become a tool of routine use to obtain more detailed vascular information.[19-21] However, its inability to provide information about the osseous structures surrounding the lesions is a significant disadvantage compared with CT angiography.[22,23] DynaCT digital angiography, reported herein, could simultaneously reconstruct and display both the osseous and contrast-filled vessels obtained from only nonsubtracted rotational data with a single injection of contrast material, which is multiply used to generate the 3D DSA images. In our study, several techniques were used to obtain high-quality images: the thin-section MIP method for reformation, a 1240 × 960 matrix, and a selected field of view. These techniques probably contributed to the improved visualization of DAVFs. Compared with 2D DSA, DynaCT could clearly demonstrate the hemodynamic features of DAVFs and the anatomic details of the fistulous points in relationship to the surrounding osseous structures more precisely.

In the treatment of CS DAVFs, overpacking of the sinus may induce a cranial nerve palsy[24] and may require more coils. In our study, the additional information provided by DynaCT

digital angiograms, such as the location of the fistulous points, was useful for following treatment of the CS DAVFs. With regard to the treatment strategy, after selective occlusion of the retrograde venous drainage outflows as the initial step, the compartment of the CS involved in the fistulous points was tightly packed with coils, and the remaining parts were loosely packed. The information from DynaCT digital angiograms (ie, the detection of the fistulous points) thus helped to prevent the overpacking of the CS. In the future, detecting the fistulous points precisely may be able to make the targeted compartmental embolization of the fistulous points. For tentorial DAVFs, the fistulous point was completely obliterated because DynaCT precisely delineated the topographic relationship between the hemodynamic features of the DAVF and the surrounding osseous structures. For endovascular treatment as well as other treatments of DAVFs, detecting the fistulous points precisely and their complete obliteration could increase the rates of an anatomic and clinical cure.

There were some limitations in this study. First, the image quality of DynaCT digital angiogram was not directly compared with that of the currently used 3D DSA. Additional investigations must be performed to evaluate the superiority to diagnose DAVFs. Second, the results were acquired from a small number of patients. Nevertheless, the results warrant additional investigations in a larger number of patients with DAVFs to assess the value of DynaCT. Finally, DynaCT imaging may not always distinguish the feeding arteries from the draining veins because of limitations in the dynamic assessment for the cerebral circulation. It might be better to evaluate the anatomic significance of these structures in conjunction with 2D or 3D DSA images.

Conclusions

Our study demonstrated that compared with 2D DSA, DynaCT digital angiography provides more detailed information for the evaluation of DAVFs. DynaCT digital angiography provides a high contrast and isotropic spatial resolution, thus allowing a reliable visualization of small vessels and fine osseous structures. Such detailed information, especially for the fistulous points, could be very useful for either the endovascular or the surgical treatments of DAVFs.

Acknowledgments

We thank Yoshisada Shibata, PhD, and Reiko Ideguchi, MD, for their critical review of the manuscript and outstanding professional guidance.

References

1. Barrow DL, Spector RH, Braun IF, et al. **Classification and treatment of spontaneous carotid-cavernous sinus fistulas.** *J Neurosurg* 1985;62:248–56
2. Kiyosue H, Tanoue S, Okahara M, et al. **Recurrence of dural arteriovenous fistula in another location after selective transvenous coil embolization: report of two cases.** *AJNR Am J Neuroradiol* 2002;23:689–92
3. Lasjaunias P, Chiu M, ter Brugge K, et al. **Neurological manifestations of intracranial dural arteriovenous malformations.** *J Neurosurg* 1986;64:724–30
4. Roy D, Raymond J. **The role of transvenous embolization in the treatment of intracranial dural arteriovenous fistulas.** *Neurosurgery* 1997;40:1133–41
5. Ushikoshi S, Houkin K, Kuroda S, et al. **Surgical treatment of intracranial dural arteriovenous fistulas.** *Surg Neurol* 2002;57:253–61
6. Guo WY, Pan DH, Wu HM, et al. **Radiosurgery as a treatment alternative for dural arteriovenous fistulas of the cavernous sinus.** *AJNR Am J Neuroradiol* 1998;19:1081–87
7. Goto K, Sidipratomo P, Ogata N, et al. **Combining endovascular and neurosurgical treatments of high-risk dural arteriovenous fistulas in the lateral sinus and the confluence of the sinuses.** *J Neurosurg* 1999;90:289–99
8. Link MJ, Coffey RJ, Nichols DA, et al. **The role of radiosurgery and particulate embolization in the treatment of dural arteriovenous fistulas.** *J Neurosurg* 1996;84:804–09
9. Kiyosue H, Hori Y, Okahara M, et al. **Treatment of intracranial dural arteriovenous fistulas: current strategies based on location and hemodynamics, and alternative techniques of transcatheter embolization.** *Radiographics* 2004;24:1637–53
10. Meckel S, Maier M, Ruiz DS, et al. **MR angiography of dural arteriovenous fistulas: diagnosis and follow-up after treatment using a time-resolved 3D contrast-enhanced technique.** *AJNR Am J Neuroradiol* 2007;28:877–84
11. Horie N, Morikawa M, Kitigawa N, et al. **2D thick-section MR digital subtraction angiography for the assessment of dural arteriovenous fistulas.** *AJNR Am J Neuroradiol* 2006;27:264–69
12. Orth RC, Wallace MJ, Kuo MD. **C-arm cone-beam CT: general principles and technical considerations for use in interventional radiology.** *J Vasc Interv Radiol* 2008;19:814–20
13. Harris FS, Rhoton AL. **Anatomy of the cavernous sinus. A microsurgical study.** *J Neurosurg* 1976;45:169–80
14. Picard L, Bracard S, Islak C, et al. **Dural fistulae of the tentorium cerebelli. Radioanatomical, clinical and therapeutic considerations.** *J Neuroradiol* 1990;17:161–81
15. Aoki S, Yoshikawa T, Hori M, et al. **MR digital subtraction angiography for the assessment of cranial arteriovenous malformations and fistulas.** *AJR Am J Roentgenol* 2000;175:451–53
16. Noguchi K, Melhem ER, Kanazawa T, et al. **Intracranial dural arteriovenous fistulas: evaluation with combined 3D time-of-flight MR angiography and MR digital subtraction angiography.** *AJR Am J Roentgenol* 2004;182:183–90
17. Heiserman JE, Dean BL, Hodak JA, et al. **Neurologic complications of cerebral angiography.** *AJNR Am J Neuroradiol* 1994;15:1401–07
18. Willinsky RA, Taylor SM, TerBrugge K, et al. **Neurologic complications of cerebral angiography: prospective analysis of 2,899 procedures and review of the literature.** *Radiology* 2003;227:522–28
19. Sugahara T, Korogi Y, Nakashima K, et al. **Comparison of 2D and 3D digital subtraction angiography in evaluation of intracranial aneurysms.** *AJNR Am J Neuroradiol* 2002;23:1545–52
20. Abe T, Hirohata M, Tanaka N, et al. **Clinical benefits of rotational 3D angiography in endovascular treatment of ruptured cerebral aneurysm.** *AJNR Am J Neuroradiol* 2002;23:686–88
21. Prestigiacomo CJ, Niimi Y, Setton A, et al. **Three-dimensional rotational spinal angiography in the evaluation and treatment of vascular malformations.** *AJNR Am J Neuroradiol* 2003;24:1429–35
22. Chappell ET, Moure FC, Good MC. **Comparison of computed tomographic angiography with digital subtraction angiography in the diagnosis of cerebral aneurysms: a meta-analysis.** *Neurosurgery* 2003;52:624–31
23. Hirai T, Korogi Y, Ono K, et al. **Preoperative evaluation of intracranial aneurysms: usefulness of intraarterial 3D CT angiography and conventional angiography with a combined unit–initial experience.** *Radiology* 2001;220:499–505
24. Agid R, Willinsky RA, Haw C, et al. **Targeted compartmental embolization of cavernous sinus dural arteriovenous fistulae using transfemoral medial and lateral facial vein approaches.** *Neuroradiology* 2004;46:156–60